Resonance with Respect to Angular Positions of an Unbalance of a Cracked Rotor in a Nonlinear Rotor System

Feng Lu and Nong Zhang

Mechanical and Manufacturing Engineering Group, Faculty of Engineering, University of Technology Sydney, PO Box 123 Broadway, Sydney, NSW 2007, Australia

(Received 28 November 2000; accepted 29 November 2001)

Cracked rotors have nonlinear spring characteristics of a piecewise linear type due to an open-closed mechanism of cracks. There have been many studies on the dynamic behaviour of cracked rotors in order to develop fault diagnosis systems for detecting cracks. However, most of these studies concern the change in resonance phenomena mainly due to cracks in rotor systems with linear supports. In many practical rotor systems, various kinds of nonlinear spring characteristics may exist due to mechanical elements, such as nonlinear bearing supports, and the rotor systems become nonlinear. Therefore, existing fault diagnosis systems are unable to detect cracks in such nonlinear rotor systems which are supported by nonlinear bearings. In this paper, we study the vibrational behaviour of a cracked rotor with nonlinear bearing supports and focus on the effect of combined resonances caused by a crack and nonlinear bearing supports. In particular, we investigate in detail the resonance phenomena of a harmonic resonance and a 1/2-order subharmonic resonance by numerical simulations using a PWL model and theoretical solutions using a PS model. The results show that the dynamic behaviours of a cracked rotor in a nonlinear rotor system are obviously different from those in a rotor system with linear supports, and the change in vibrational behaviour of a harmonic resonance and a 1/2-order subharmonic resonance are significant due to changes of angular positions of an unbalance.

1. INTRODUCTION

Transverse cracks due to fatigue in rotor shafts are one of the most serious causes of accidents in rotating machinery. A detailed investigation into the vibrations of cracked rotors is very important for developing a fault diagnosis system and detecting rotor cracks. In order to find a method for detecting cracks in rotating shafts, the dynamic behaviour of cracked rotors has been studied since the middle of the 1970s. Most of the early research results were well summarised in a book by Dimarogonas and Pafelias[1] and more literature on the dynamics of cracked rotor systems was presented in a review paper by Wauer[2], and more recently, a survey on simple cracked rotors and a review on general cracked structures were given by Gasch[3] and Dimarogonas[4], respectively.

There are two major research fields in the study of dynamics of cracked rotors. One is the modelling of cracked rotors and the other is the detecting of rotor cracks. In order to predict the change in vibrational behaviour due to rotor cracks, a lot of crack models have been developed. The typical model is the breathing crack model developed by Gasch[5]. Gasch[5,6] and Henry and Okah-Avae[7] firstly considered the nonlinear mechanism of a crack with different stiffnesses for the open and closed crack in a body-fixed rotating coordinate system. They presented the spring characteristics of a cracked rotor as a piecewise linear type. They made computer simulations using equations of motion with nonlinear spring characteristics of a piecewise linear type and found that the following resonances occurred in the cracked rotor: 1) a harmonic resonance at the major critical speed, 2) a super-harmonic resonance at the secondary critical speed, 3) super-harmonic resonances of orders higher than the second ($n = 3, 4$), 4) a 3/2-order super-subharmonic resonance and 5) a 1/2-order subharmonic resonance. The harmonic resonance and the 1/2-order subharmonic resonance which we discuss in this paper were also found in experiments. Mayes and Davies[8] used the Green function to calculate the compliance of a cracked rotor in a space-fixed coordinate system and correlated some experimental results with their theoretical background. In later papers, Mayes and Davies[9,10] presented an approximate method to model a cracked rotor in which the crack was simulated by a reduced diameter section and the cracked rotor was analysed in a multi-rotor-bearing system. They found that the vibrational behaviour was similar to that of a slotted shaft with additional excitation due to the opening and closing of a crack. Grabowski[11] assumed that whether the cracks are fully open, partially open or fully closed depends on the crack location in relation to the horizontal diameter of the shaft. Grabowski[12] investigated the dynamic behaviour of a realistic cracked rotor system using a model formulation and found the 1/2-order subharmonic resonance from experiments. Dimarogonas and Papadopoulos[13,14] pointed out that the crack position has a large influence on resonances, and the information of subharmonic resonances and frequency shifting are very important for crack identification. Papadopoulos and Dimarogonas[15], and Sekhar and Balaji[16] used the first four terms of a Fourier cosine series to express the stiffness variation of the cracked rotor. Gasch[17] and Tamura[18] investigated the dynamic behaviour of a cracked rotor and solved the equations of motion of a parametrically-excited system. The solution was obtained by linearising the spring characteristics of the cracked rotor. In this study, they could not obtain the solution for the steady-state oscillations that were observed in the simulations by Gasch[5,6]. Ishida et al.[19,20] approximated the nonlinear restoring force of a cracked rotor by a power series model and presented the detailed results obtained from theoretical analyses, numerical simulations and experiments. Nelson and Nataraj[21], and Sekhar and Balaji[16] analysed the dynamic behaviour of a cracked rotor system using finite element methods. Meng and Hahn[22] analysed the rotor system with small cracks and small vibrations theoretically and numerically. Iman et al.[23] presented a very successful on-line crack detection method which is based on the vibration signature analysis approach. This can be applied to detect incipient transverse cracks in the turbine-generator, pumps and motors. The on-line crack detection methods depend mainly on rotor acceleration and deceleration in the subcritical speed range. Ratan et al.[24] developed a new method to detect the existence and location of cracks in rotating shafts. This method is based on obtaining the Fourier transform of the response of the cracked rotor. Chan and Lai[25] investigated the vibrations of a cracked rotor in turbomachinery by numerical simulations and found that the resonances occurred at one-half and one-third subcritical speeds.

The effects of angular positions of an unbalance on resonance have been studied in many published papers. Henry and Okah-Avae[7] found that the resonance amplitude depends on the direction of unbalance of cracked rotors. Gasch[5], Dimarogonas and Papadopoulos[13,14] explained the change in the synchronous amplitude and phase angle, and presented the results of the influence of crack positions on the resonance. Davies and Mayes[9,10] showed that the crack opening and closing is a function of the bending moment at the crack position, and the principal axis and the stiffness change are a function of the instantaneous area of the crack. They obtained some results from experiments and described the effects of angular positions of an unbalance on vibrational behaviour of the cracked rotor system. Ishida et al.[19] investigated in detail the changes in resonance curves due to angular positions of an unbalance at the major critical speed.

The cracked rotor has nonlinear spring characteristics of a piecewise linear type due to an open-closed mechanism of cracks. Most studies concern the vibrations that take place mainly due to cracks in rotor systems with linear supports. In rotating machinery, there exist nonlinear characteristics in the restoring forces or damping forces for various reasons, such as clearance in ball bearings, oil film in journal bearings and so on.[26-29] Consequently, the existing vibration fault diagnostic techniques developed based on cracked rotor with linear supports have the limitation that they cannot be used to detect cracks in cracked rotor systems with nonlinear supports.

The dynamic behaviour of cracked rotors with bearing supports has been studied. Okah-Avae[30-31] simulated a rotor system containing a transverse crack and hydrodynamic bearing supports using a four degree of freedom model and concluded that the model can be reduced to a two degrees of freedom model by assuming that the rotor is rigidly supported. Müller et al.[32] used a model-based method to establish a clear relation between cracks in turbo rotors and vibration effects measured in journal bearings. Tamura[18] and Gasch[3] analysed the stability of a cracked rotor supported on rigid bearings. Meng and Gasch[33] first published the paper about the stability and stability degree of a cracked flexible rotor supported on different journal bearings. Ishida and Lu[34], and Lu and Zhang[35] studied the vibrational behaviour of a rotor system with a crack and nonlinear bearing supports. Until now the effects of nonlinear combined resonances caused by the crack and the nonlinear supports have been investigated in only a few papers.

In this paper, we consider that the rotor system has both the nonlinearity due to a crack and the nonlinearity due to bearing supports. We study the dynamic behaviour of a cracked rotor by numerical simulations using a piecewise linear model and focus on the effects of nonlinear combined resonances, which are caused by a crack and bearing supports. For the theoretical solution, we have obtain the nonlinear equations of motion of a cracked rotor system by approximating its piecewise linear spring characteristics using a power series model. In addition, we investigate in detail the vibrational behaviour of the harmonic resonance at the major critical speed and the 1/2-order subharmonic resonance in a cracked rotor system with nonlinear supports. The results of this research are useful for developing vibration fault diagnostic techniques for cracked rotor systems in rotating machinery which are supported by nonlinear bearings.

2. NONLINEAR SPRING CHARACTERISTICS AND EQUATIONS OF MOTION

2.1. Model of a Cracked Rotor

Figure 1 shows a two degree of freedom model of the inclination oscillation of a cracked rotor system, which is installed horizontally and supported by nonlinear bearings. In this model, an elastic massless shaft carries a disk which is mounted at the middle of the shaft. The inclination angle of the shaft at the position of the disk is denoted by θ. We adopt a static rectangular coordinate system $0-xyz$ in which the z-axis coincides with the bearings centre line. We also utilise a new static rectangular coordinate system $0-\theta_x\theta_y$ in which θ_x and θ_y are the projections of θ onto the xz and yz-planes, respectively. In addition, we define the rotating coordinate system $0-x'y'z'$ in which the x'-axis coincides with the direction of the boundary of the crack. We also utilise a new rotating coordinate $0-\theta_x'\theta_y'$ which makes use of the projections of θ onto the $x'z$ and $y'z$-planes. We consider that the cracked rotor system has two kinds of nonlinearity. One is the nonlinearity caused by the crack, the other is the nonlinearity due to the bearing supports.

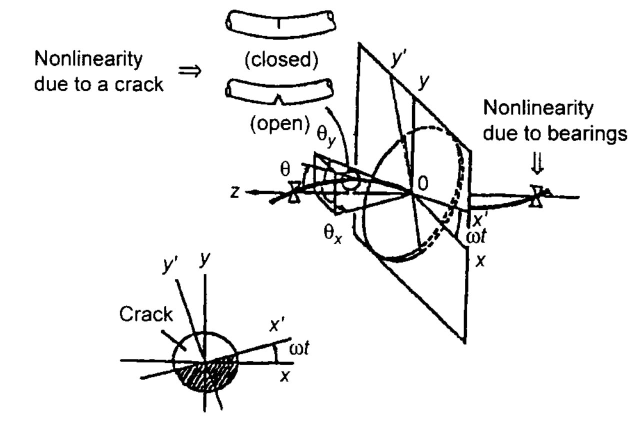

Figure 1. Model of a cracked rotor and coordinate systems.

2.2. Nonlinearity Due to a Crack

We study the dynamic behaviour of a cracked rotor using the model of a breathing crack which has been widely used for qualitative vibrational analysis of cracked rotor systems. The model is simple but still can represent the most important characteristics of the cracked rotor. Figure 2 shows the nonlinearity due to a crack. In this model, the stiffness of a cracked rotor changes due to the mechanism of the open-closed crack. The shaft stiffness becomes small when the crack opens, i.e., $\theta'_y > 0$, and large when the crack closes, i.e., $\theta'_y < 0$. Consequently, the spring characteristics in the θ'_y-direction have a nonlinearity of a piecewise linear type whilst the spring characteristics in the θ'_x-direction are linear. The nonlinear spring characteristics due to a crack can be expressed as follows:

$$\begin{aligned} -M'_x &= k'_1\theta'_x; \\ -M'_y &= (k'_2 - \Delta k'_2)\theta'_y \ (\theta'_y > 0); \\ -M'_y &= (k'_2 + \Delta k'_2)\theta'_y \ (\theta'_y < 0), \end{aligned} \tag{1}$$

where, M'_x and M'_y are the components of the restoring moments in the $x'z$ and $y'z$-planes respectively. We can obtain the restoring moments in the xy and yz-planes from these expressions. We call the model represented by Eq. (1) a piecewise linear model (PWL model) of the cracked rotor. As these expressions are inconvenient in the analysis, we can also model these spring characteristics approximately using the following power series, up to the fourth order:

$$\begin{aligned} -M'_x &= k'_x\theta'_x; \\ -M'_y &= k'_y\theta'_y + \varepsilon_2\theta'^2_y + \beta_3\theta'^3_y + \varepsilon_4\theta'^4_y. \end{aligned} \tag{2}$$

We neglect the coefficient β_3 in the following analyses because β_3 is much smaller than ε_2 and ε_4. This conclusion has been found from experiments. We call the model represented by Eq. (2) a power series model (PS model) of the cracked rotor.[19,20]

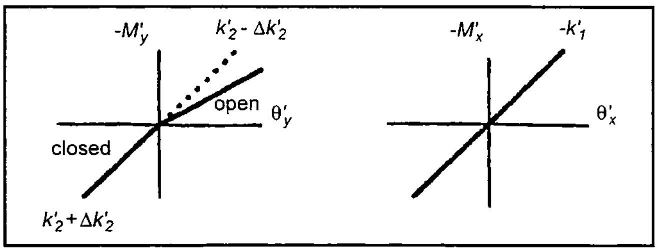

Figure 2. Nonlinear spring characteristics of a crack.

2.3. Nonlinearity Due to Bearing Supports

There are various kinds of nonlinearity in the restoring forces of rotor systems. The nonlinear spring characteristics due to bearing supports have been studied widely. In order to derive the most general expression of nonlinear terms, Yamamoto et al.[36,37] modelled the nonlinear spring characteristics by a power series approximation and presented an expression of nonlinear spring characteristics due to bearing supports from the corresponding potential energy. In a two degree of freedom model system, if we consider the sum of the nonlinear terms up to the third power of the coordinates θ_x and θ_y, the corresponding potential energy V of the rotor system can be expressed as follows:

$$V = V_0 + V_N = \frac{1}{2}\left(\theta_x^2 + \theta_y^2\right) + \sum_{(i+j=3)} \varepsilon_{ij}\theta_x^i\theta_y^j + \sum_{(i+j=4)} \beta_{ij}\theta_x^i\theta_y^j, \tag{3}$$

where, V_0 and V_N are the components corresponding to the linear and nonlinear terms in the restoring forces, and where $\varepsilon_{ij}(i+j=3)$ and $\beta_{ij}(i+j=4)$ represent the coefficients of the nonlinear unsymmetrical and symmetrical terms, respectively. Using the transformation $\theta_x = \theta\cos\varphi, \theta_y = \theta\sin\varphi$, we can transform Eq. (3) into the polar coordinate expression:

$$\begin{aligned} V = &\frac{1}{2}\theta^2 + \left(\varepsilon_c^{(1)}\cos\varphi + \varepsilon_s^{(1)}\sin\varphi + \varepsilon_c^{(3)}\cos 3\varphi + \varepsilon_s^{(3)}\sin 3\varphi\right)\theta^3 + \\ &\left(\beta^{(0)} + \beta_c^{(2)}\cos 2\varphi + \beta_s^{(2)}\sin 2\varphi + \beta_c^{(4)}\cos 4\varphi + \beta_s^{(4)}\sin 4\varphi\right)\theta^4 = \\ &\frac{1}{2}\theta^2 + [\varepsilon^{(1)}\cos(\varphi-\varphi_1) + \varepsilon^{(3)}\sin 3(\varphi-\varphi_3)]\theta^3 + \\ &[\beta^{(0)} + \beta^{(2)}\cos 2(\varphi-\varphi_2) + \beta^{(4)}\cos 4(\varphi-\varphi_4)]\theta^4, \end{aligned} \tag{4}$$

where, the coefficients of the nonlinear terms $\varepsilon^{(n)}$ and $\beta^{(n)}$ represent the nonlinear components whose magnitude changes n times $(n = 0, 1, 2, 3, 4)$, while the direction angle φ changes its value from 0 to 2π but at the same time θ is kept constant. We designate these nonlinear components by the notation $N(n)$ $(n = 0, 1, 2, 3, 4)$. Here $N(0), N(2), N(4)$ express the nonlinear symmetrical components and $N(1), N(3)$ express the nonlinear unsymmetrical components, respectively. A detailed explanation of the nonlinear spring characteristics due to bearing supports can be found in the references[28,29,37]. The definitions of the non-dimensional parameters in Eqs. (1)-(4) are given in the following section.

2.4. Equations of Motion

In rotor systems with no cracks and no nonlinear bearing supports, the equations of motion of the inclination oscillation can be written as follows:

$$\begin{aligned} I\ddot{\theta}_x + I_p\omega\dot{\theta}_y + c\dot{\theta}_x + k\theta_x &= (I - I_p)\tau\omega^2\cos\omega t; \\ I\ddot{\theta}_y - I_p\omega\dot{\theta}_x + c\dot{\theta}_y + k\theta_y &= (I - I_p)\tau\omega^2\sin\omega t + M_0. \end{aligned} \tag{5}$$

We assume that a cracked rotor has nonlinearity due to a crack and nonlinearity due to bearing supports in Fig. 1. Let the magnitude and the angular position of the dynamic unbalance be τ and α, the polar and diametrical moment of inertia of the rotor be I_p and I and their ratio be i_p, the rotational speed be ω, the damping coefficient be c, the bending stiffness of a shaft be k, and the time be t, respectively. Here we introduce the representative angle τ_0 whose magnitude is of the same order as the amplitude of the oscillation. We consider a constant moment M_0 in θ_y-direction, which corresponds to the gravitational force. Using the following dimensionless quantities:

$$\theta_x' = \frac{\theta_x}{\tau_0}; \theta_y' = \frac{\theta_y}{\tau_0}; \tau' = \frac{\tau}{\tau_0}; i_p = \frac{I_p}{I}; c' = \frac{c}{\sqrt{kI}}; t' = t\sqrt{\frac{k}{I}}$$

$$\omega' = \omega\sqrt{\frac{I}{k}}; M_0' = \frac{M_0}{k\tau_0}; n_{\theta_x}' = \frac{n_{\theta_x}}{k\tau_0}; n_{\theta_y}' = \frac{n_{\theta_y}}{k\tau_0}; N_{\theta_x}' = \frac{N_{\theta_x}}{k\tau_0};$$

$$N_{\theta_y}' = \frac{N_{\theta_y}}{k\tau_0}; \Delta_1' = \frac{\Delta\delta_1}{\delta}; \Delta_2' = \frac{\Delta\delta_2}{\delta}; \delta = \frac{k_1' + k_2'}{2};$$

$$\Delta\delta_1 = \frac{k_1' - k_2'}{2}; \Delta\delta_2 = \frac{\Delta k_2'}{2}; \Delta' = \frac{(k_x' - k_y')}{(k_x' + k_y')}, \quad (6)$$

we can obtain two sets of nonlinear equations of motion for a cracked rotor system with both (a) nonlinearity due to a crack and (b) nonlinearity due to bearing supports. The first is the two equations of motion of the cracked rotor system make use of a piecewise linear model, which is used for numerical simulations. Concerning the double sign, the upper signs and the lower signs are used for $\theta_y' > 0$ and $\theta_y' < 0$, and the equations of motion of a PWL model are obtained from Eqs. (1) and (5) as follows:[19,35]

$$\ddot{\theta}_x + i_p\omega\dot{\theta}_y + c\dot{\theta}_x + (1 \mp \Delta_2)\theta_x +$$
$$(\Delta_1 \pm \Delta_2)(\theta_x C_2 + \theta_y S_2) + n_{\theta_x} = M\cos(\omega t + \alpha);$$
$$\ddot{\theta}_y - i_p\omega\dot{\theta}_x + c\dot{\theta}_y + (1 \mp \Delta_2)\theta_y +$$
$$(\Delta_1 \pm \Delta_2)(\theta_x S_2 - \theta_y C_2) + n_{\theta_y} = M\sin(\omega t + \alpha) + M_0. \quad (7)$$

The second set is the equations of motion of the cracked rotor system. They utilise a power series model which is used for the theoretical solutions. The equations of motion of a PS model are obtained from Eqs. (2) and (5) as follows:[19,35]

$$\ddot{\theta}_x + i_p\omega\dot{\theta}_y + c\dot{\theta}_x + \theta_x + \Delta(\theta_x C_2 + \theta_y S_2) +$$
$$N_{\theta_x} + n_{\theta_x} = M\cos(\omega t + \alpha);$$
$$\ddot{\theta}_y - i_p\omega\dot{\theta}_x + c\dot{\theta}_y + \theta_y + \Delta(\theta_x S_2 - \theta_y C_2) +$$
$$N_{\theta_y} + n_{\theta_y} = M\sin(\omega t + \alpha) + M_0, \quad (8)$$

where the prime $'$ is omitted. In these expressions, the symbols $S_n = \sin n\omega t, C_n = \cos n\omega t$, and $M = (1 - i_p)\tau\omega^2$ are used for simplicity. Δ_1, Δ_2 and Δ express the directional difference in the shaft stiffness of the cracked rotor. A detailed derivation for Eqs. (7) and (8) can be found in the books authored by Yamamoto and Ishida[28,29], here the nonlinear terms due to bearing supports have been added. The nonlinear terms $N_{\theta x}$ and $N_{\theta y}$ due to a crack are represented as follows:

$$N_{\theta_x} = \frac{\varepsilon_2}{4}\left[(-3S_1 + S_3)\theta_x^2 + 2(C_1 - C_3)\theta_x\theta_y - (S_1 + S_3)\theta_y^2\right] +$$
$$\frac{\varepsilon_4}{16}\left[-(10S_1 - 5S_3 + S_5)\theta_x^4 + 4(2C_1 - 3C_3 + C_5)\theta_x^3\theta_y -\right.$$
$$6(2S_1 + S_3 - S_5)\theta_x^2\theta_y^2 + 4(2C_1 - C_3 - C_5)\theta_x\theta_y^3 -$$
$$\left.(2S_1 + 3S_3 + S_5)\theta_y^4\right];$$
$$N_{\theta_y} = \frac{\varepsilon_2}{4}\left[(C_1 - C_3)\theta_x^2 - 2(S_1 + S_3)\theta_x\theta_y + (3C_1 + C_3)\theta_y^2\right] +$$
$$\frac{\varepsilon_4}{16}\left[(2C_1 - 3C_3 + C_5)\theta_x^4 - 4(2S_1 + S_3 - S_5)\theta_x^3\theta_y +\right.$$
$$6(2C_1 - C_3 - C_5)\theta_x^2\theta_y^2 - 4(2S_1 + 3S_3 + S_5)\theta_x\theta_y^3 +$$
$$\left.(10C_1 + 5C_3 + C_5)\theta_y^4\right]. \quad (9)$$

If we consider the nonlinear terms up to the third order, we can obtain the nonlinear terms $n_{\theta x}$ and $n_{\theta y}$ due to bearing supports as in the following expression:

$$n_{\theta_x} = \frac{\partial V_N}{\partial \theta_x} = 3\varepsilon_{30}\theta_x^2 + 2\varepsilon_{21}\theta_x\theta_y + \varepsilon_{12}\theta_y^2 +$$
$$4\beta_{40}\theta_x^3 + 3\beta_{31}\theta_x^2\theta_y + 2\beta_{22}\theta_x\theta_y^2 + \beta_{13}\theta_y^3;$$
$$n_{\theta_y} = \frac{\partial V_N}{\partial \theta_y} = \varepsilon_{21}\theta_x^2 + 2\varepsilon_{12}\theta_x\theta_y + 3\varepsilon_{03}\theta_y^2 +$$
$$\beta_{31}\theta_x^3 + 2\beta_{22}\theta_x^2\theta_y + 3\beta_{13}\theta_x\theta_y^2 + 4\beta_{04}\theta_y^3. \quad (10)$$

3. NUMERICAL SIMULATIONS

In order to investigate the dynamic behaviour of a cracked rotor in a nonlinear rotor system, we carry out numerical simulations with a PWL model and focus on the resonance with respect to the angular positions of an unbalance.

3.1. 1/2-Order Subharmonic Resonance

Resonance curves for a cracked rotor in a linear rotor system. Figure 3 shows the resonance curves of 1/2-order

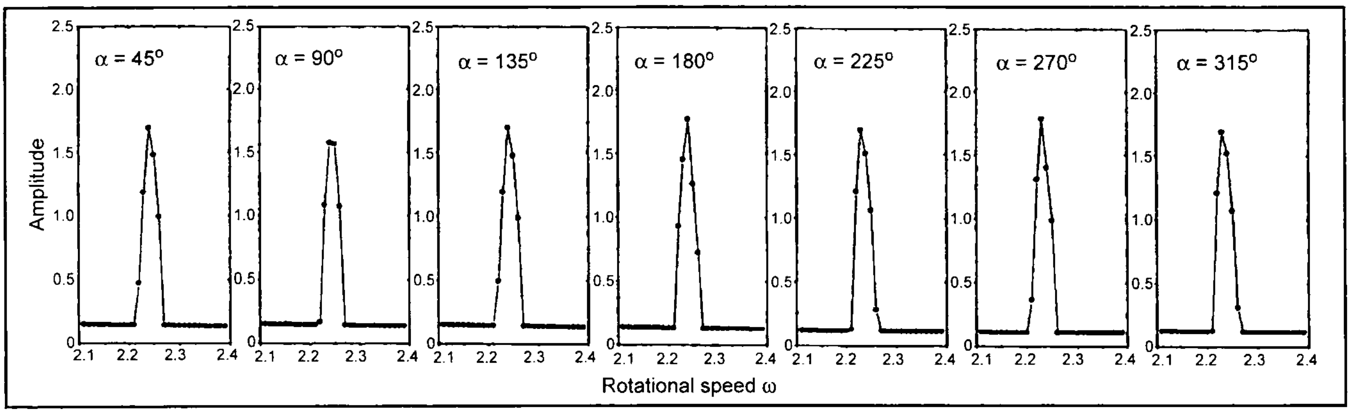

Figure 3. 1/2-Order subharmonic resonance with respect to angular positions in a linear rotor system ($i_p = 0.1, c = 0.02, \tau = 0.1, \Delta_1 = \Delta_2 = 0.05, M_0 = -1.0$).

subharmonic resonance due to nonlinearity of a crack, where $\tau = 0.1, i_p = 0.1, c = 0.02, M_0 = -1.0, \Delta_1 = \Delta 2 = 0.05$ and ω is the non-dimensional rotating speed. In this case, the resonance curves due to a crack are almost the same for different angular positions of an unbalance.

Resonance curves of a cracked rotor in a nonlinear rotor system. The resonance curves of 1/2-order subharmonic resonance are shown in Figs. 4 and 5, where the nonlinear components $\varepsilon_c^{(1)} = \varepsilon_s^{(1)} = 0.02$ in Fig. 4(a), $\varepsilon_c^{(1)} = \varepsilon_s^{(1)} = 0.03$ in Fig. 4(b), $\beta_c^{(2)} = \beta_s^{(2)} = 0.004$ in Fig. 5(a), and $\beta_c^{(2)} = \beta_s^{(2)} = 0.012$

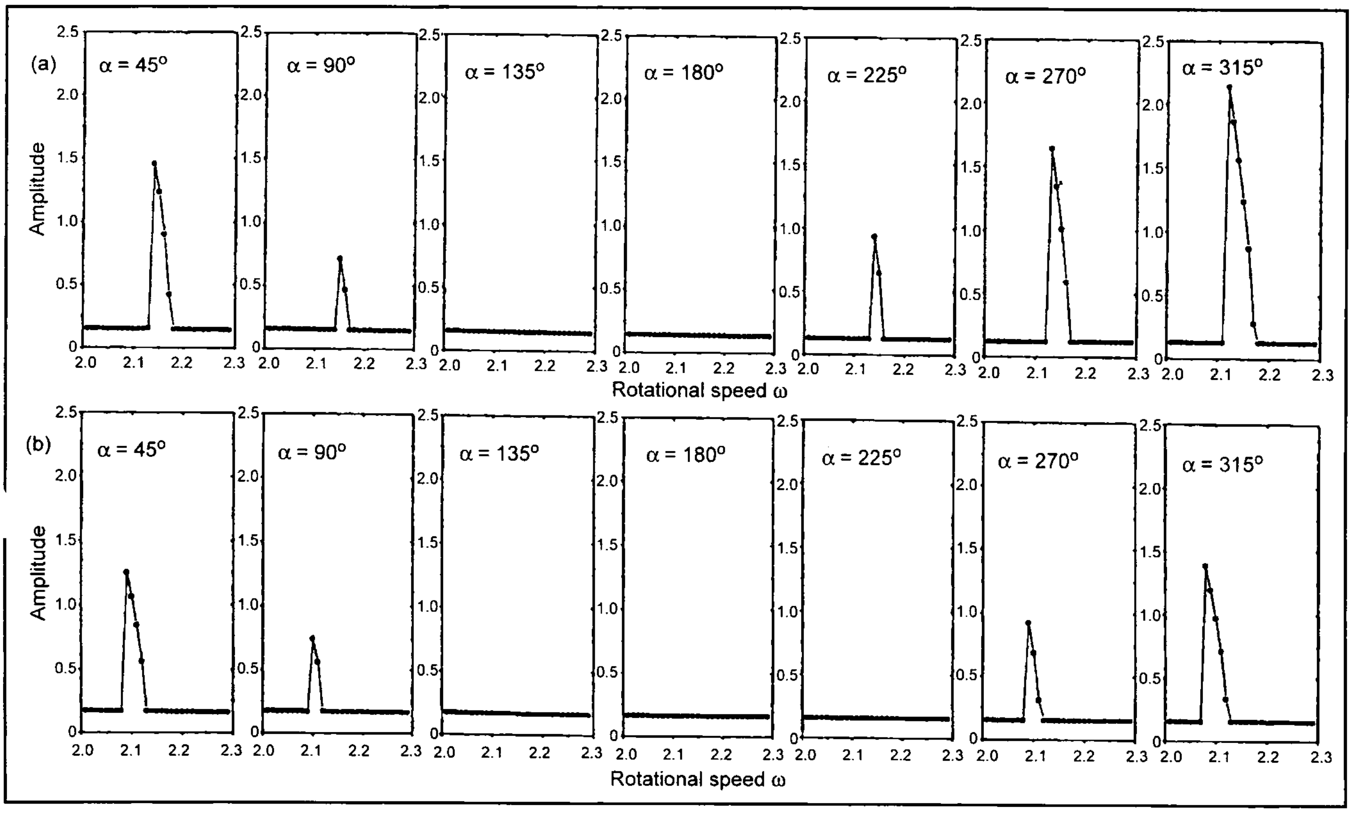

Figure 4. 1/2-Order subharmonic resonance with respect to angular positions in a nonlinear rotor system ($i_p = 0.1, c = 0.02, \tau = 0.1, \Delta_1 = \Delta_2 = 0.05, M_0 = -1.0$). (a) $\varepsilon_c^{(1)} = \varepsilon_s^{(1)} = 0.02$; (b) $\varepsilon_c^{(1)} = \varepsilon_s^{(1)} = 0.03$.

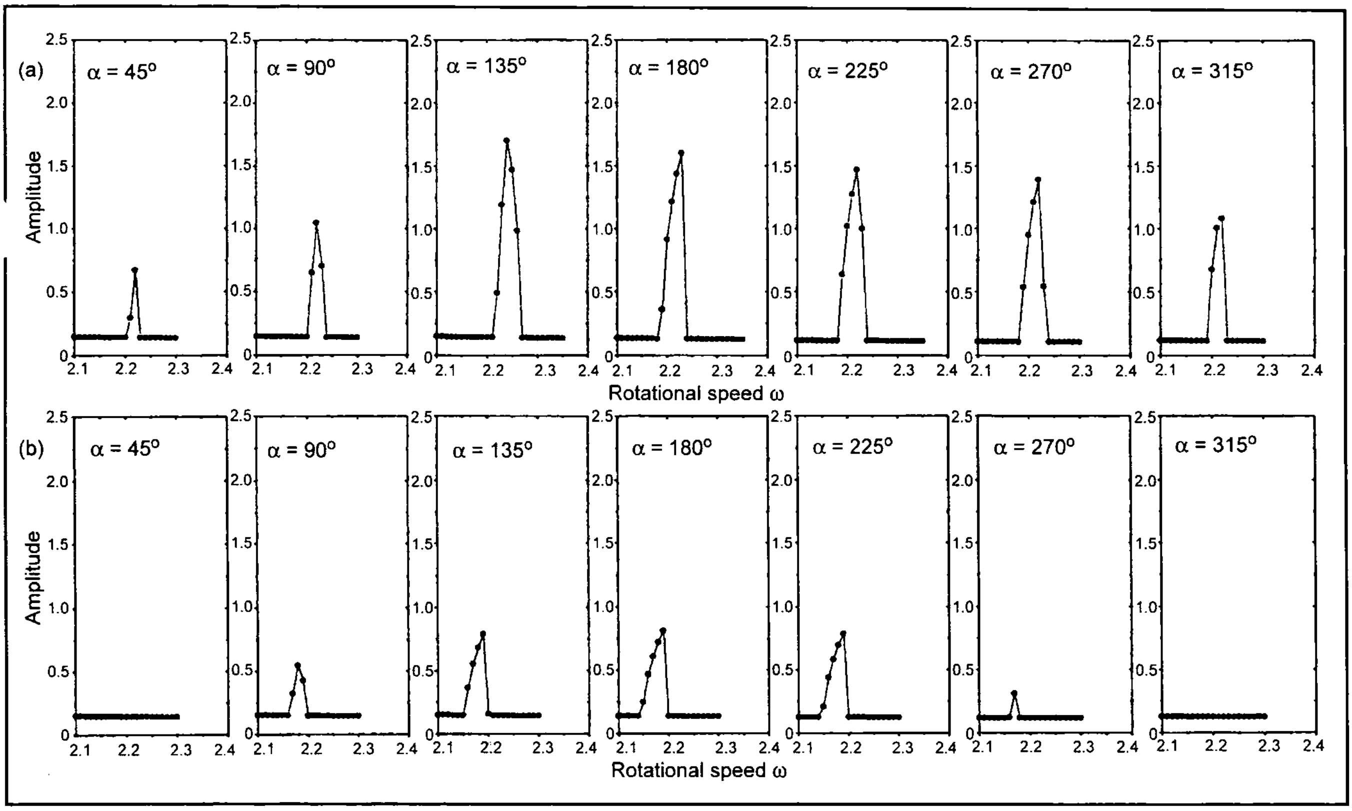

Figure 5. 1/2-Order subharmonic resonance with respect to angular positions in a nonlinear rotor system ($i_p = 0.1, c = 0.02, \tau = 0.1, \Delta_1 = \Delta_2 = 0.05, M_0 = -1.0$). (a) $\beta_c^{(2)} = \beta_s^{(2)} = 0.004$; (b) $\beta_c^{(2)} = \beta_s^{(2)} = 0.012$.

in Fig. 5(b), respectively. Comparing these results to those in Fig. 3, we can make the following observations.

1. In the case of a cracked rotor with the unsymmetrical nonlinear component $N(1)$ ($\varepsilon_c^{(1)} = \varepsilon_s^{(1)} \neq 0$), a) the resonance amplitudes have different magnitudes for different angular position; b) the resonance amplitudes decrease or may disappear as $N(1)$ increases. When $\varepsilon_c^{(1)} = \varepsilon_s^{(1)} = 0.02$ in Fig. 4(a), the amplitudes first disappear at $\alpha = 135°, 180°$, and when $\varepsilon_c^{(1)} = \varepsilon_s^{(1)} = 0.03$ in Fig. 4(b), the amplitudes disappear at $\alpha = 135°, 180°, 225°$ and decrease at $\alpha = 45°, 90°, 270°, 315°$; c) the resonance curves due to different angular positions shift to the lower speed side. For example in the case of an angle $\alpha = 270°$, when the cracked rotor has no nonlinearity $N(1)$, i.e., $\varepsilon_c^{(1)} = \varepsilon_s^{(1)} = 0$, the 1/2-order subharmonic resonance occurs at the rotation speed $\omega \approx 2.23$ in Fig. 3, however, when the cracked rotor has nonlinearity $N(1)$, the resonance occurs at $\omega \approx 2.13$ when $\varepsilon_c^{(1)} = \varepsilon_s^{(1)} = 0.02$ in Fig. 4(a) and $\omega \approx 2.09$ when $\varepsilon_c^{(1)} = \varepsilon_s^{(1)} = 0.03$ in Fig. 4(b).

2. In the case of a cracked rotor with symmetrical nonlinear component $N(2)$ ($\beta_c^{(2)} = \beta_s^{(2)} \neq 0$) in Figs. 5(a) and (b), the resonance curves shift to the lower speed side and as $N(2)$ increases when $\beta_c^{(2)} = \beta_s^{(2)} = 0.012$, the resonance amplitudes decrease at $\alpha = 90°, 135°, 180°, 225°, 270°$ and disappear at $\alpha = 45°, 315°$.

3.2. Harmonic Resonance at Major Critical Speed

Resonance curves of a cracked rotor in a linear rotor system. In the case of a cracked rotor with no nonlinear components due to bearing supports as shown in Fig. 6, the harmonic resonance at the major critical speed has an unstable region when $\alpha = 45°, 90°, 135°, 180°, 225°$ and does not have an unstable region when $\alpha = 270°, 315°$, where $\tau = 0.1$, $i_p = 0.7, c = 0.02, M_0 = -1.0$, and $\Delta_1 = \Delta_2 = 0.05$.

Resonance curves for a cracked rotor in a nonlinear rotor system. Figure 7 shows the resonance curves of harmonic resonance with respect to angular positions of an unbalance of the cracked rotor where the nonlinear components $\varepsilon_s^{(1)} = 0.015$ when comparing those results to the results in Fig. 6, when the cracked rotor has unsymmetrical nonlinear component $N(1)$ ($\varepsilon_s^{(1)} \neq 0$), the unstable regions of the resonance curves are seen not to exist.

4. POWER SERIES APPROXIMATION

In this section, we investigate the harmonic resonance and the 1/2-order subharmonic resonance of a cracked rotor system using a PS model, Eq. (8), of up to a fourth order approximation.

4.1. 1/2-Order Subharmonic Resonance

Assumption made for the approximate solution. In the neighbourhood of the rotational speed ω_s where the forward natural frequency p_f and the rotating speed ω have the relationship $p_f = \omega/2$, as shown in Fig. 8, the 1/2-order subharmonic resonance of a forward whirling mode occurred. We use the symbol $O(\varepsilon)$ to denote the magnitude which is of the same order as the parameter ε. An approximate solution in the accuracy of order $O(\varepsilon)$ is assumed as follows:

$$\theta_x = R\cos\theta_f + P\cos(\omega t + \beta) + \varepsilon(a\cos\theta_f + b\sin\theta_f) + A_x;$$

$$\theta_y = R\sin\theta_f + P\sin(\omega t + \beta) + \varepsilon(a'\sin\theta_f + b'\cos\theta_f) + A_y, \tag{11}$$

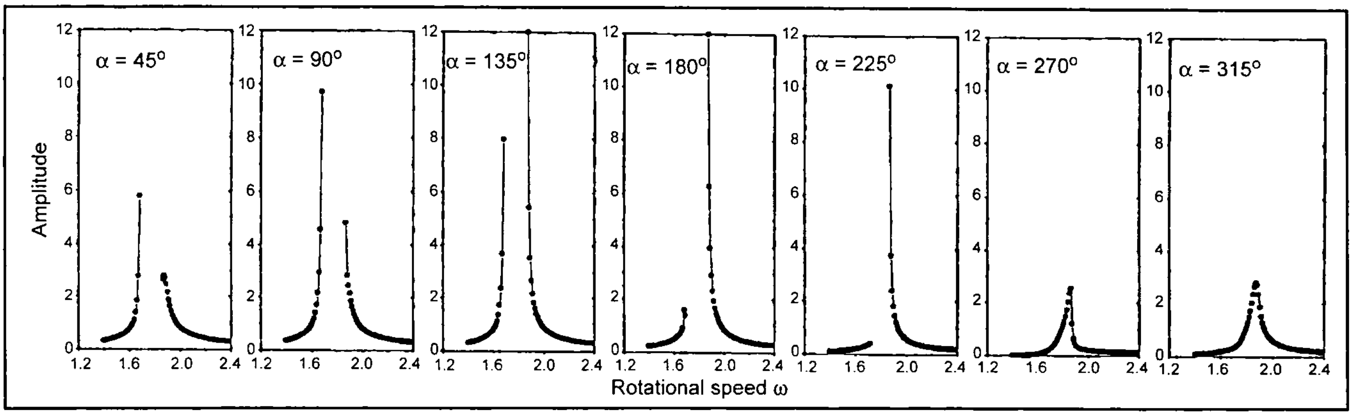

Figure 6. Harmonic resonance with respect to angular positions in a linear rotor system ($i_p = 0.7, c = 0.02, \tau = 0.1, \Delta_1 = \Delta_2 = 0.05, M_0 = -1.0$).

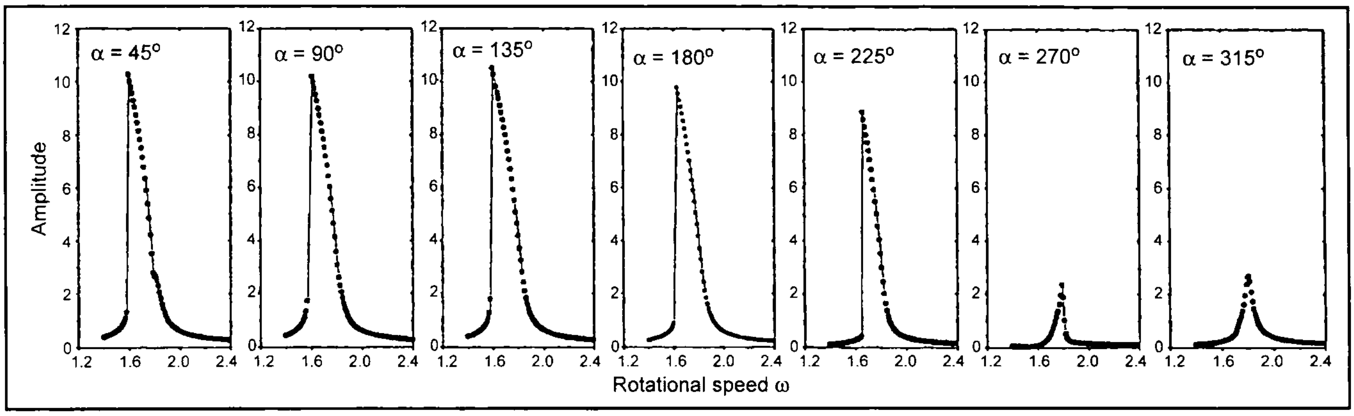

Figure 7. Harmonic resonance with respect to angular positions in a nonlinear rotor system ($i_p = 0.7, c = 0.02, \tau = 0.1, \Delta_1 = \Delta_2 = 0.05, M_0 = -1.0, \varepsilon_s^{(1)} = 0.015$).

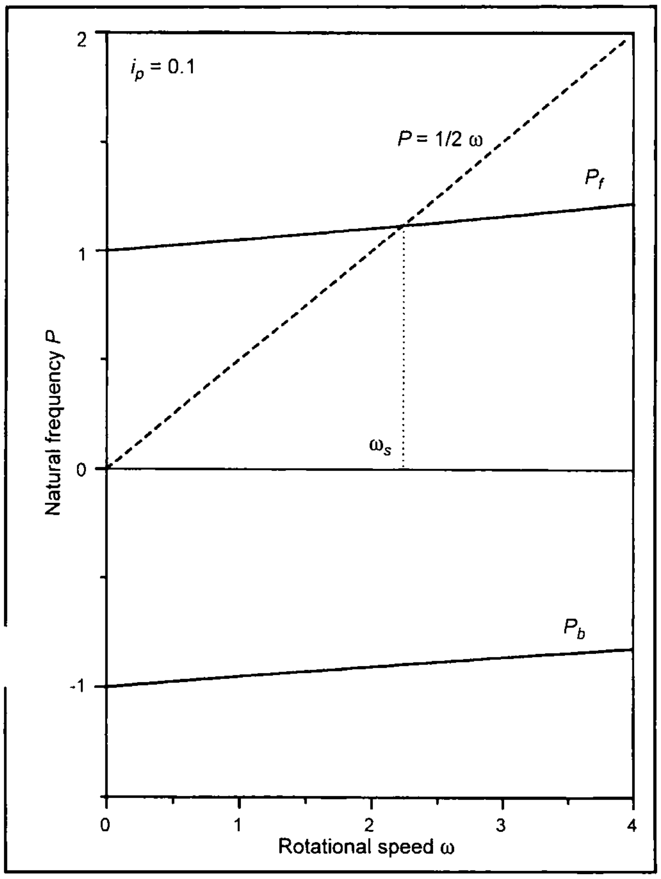

Figure 8. $p-\omega$ diagram ($i_p = 0.1$).

where $\omega_f = \omega/2$ and $\theta_f = \omega_f + \delta$. The terms with the parameter ε represent small deviations of the trajectory caused by nonlinearity. Substituting Eq. (11) into Eq. (8) and using the harmonic balance method, we can obtain the following fourth power approximation for the resonance curve:

$$0 = R_0\{-c\omega_f - 0.5\varepsilon_2 M_0 \sin 2\delta_0 - 0.25\varepsilon_4[M_0(2R_0^2 + 6P^2 + 3M_0^2)\sin 2\delta_0 - 6P_{c2}M_0 \sin 2\delta_0] + 2\varepsilon_c^{(1)} P \sin(2\delta_0 - a) - 2\varepsilon_s^{(1)} P\cos(2\delta_0 - a) - M_0 P\left(8\beta^{(0)} - 6\beta_c^{(2)}\right)\cos(2\delta_0 - a) + 6\beta_s^{(2)} M_0 P \sin(2\delta_0 - a)\};$$

$$0 = R_0\{G_f + \varepsilon_2(P\sin a - 0.5M_0 \cos 2\delta_0) + 0.25\varepsilon_4[-M_0 \times (4R_0^2 + 6P^2 + 3M_0^2)\cos 2\delta_0 + 6P_{c2}M_0\cos 2\delta_0 - 2P_{s3} + 6P_{s1}(R_0^2 + P^2 + 2M_0^2)] + 2\varepsilon_c^{(1)} P\cos(2\delta_0 - a) + 4\varepsilon_s^{(1)} M_0 + 2\varepsilon_s^{(1)} P\sin(2\delta_0 - a) + 4\beta^{(0)}(R_0^2 + 2P^2) + \left(8\beta^{(0)} - 6\beta_c^{(2)}\right)M_0^2 + \left(8\beta^{(0)} - 6\beta_c^{(2)}\right)M_0 P\sin(2\delta_0 - a) + 6\beta_s^{(2)} M_0 P\cos(2\delta_0 - a)\}, \quad (12)$$

where the symbols $P_{cn} = P^n \cos na$, $P_{sn} = P^n \sin na$ and $G_f = G(\omega_f) = 1 + i_p\omega\omega_f - \omega_f^2$ are used for simplicity. For the harmonic solution and the constant component, we adopt the approximate solutions $P = -M/G(\omega), \beta = a + \pi$ and $A_x = 0$, $A_y = M_0$ in the accuracy of $O(\varepsilon^0)$ and we can obtain a trivial solution $R_0 = 0$ and a nontrivial solution $R_0 \neq 0$. The equations include the nonlinear components $N(1)(\varepsilon_c^{(1)}, \varepsilon_s^{(1)})$, $N(2)(\beta_c^{(2)}, \beta_s^{(2)})$ and $N(0)(\beta^{(0)})$.

The results from a power series approximation. The 1/2-order subharmonic resonance curves are shown in Figs. 9 and 10, where the parameter $\tau = 0.1, a = 270°, i_p = 0.1, c = 0.015$, $M_0 = -1.0$, $\Delta = 0.05$, $\varepsilon_2 = -0.05$, $\varepsilon_4 = 0.001$. As shown in Fig. 9, when the cracked rotor does not have nonlinearity for $\varepsilon_c^{(1)} = \varepsilon_s^{(1)} = 0$, the 1/2-order subharmonic resonance occurs at the rotation speed $\omega \approx 2.24$. However, when the cracked rotor has $N(1)$, the 1/2-order subharmonic resonance occurs at $\omega \approx 2.15$ ($\varepsilon_c^{(1)} = \varepsilon_s^{(1)} = 0.02$) and $\omega \approx 2.10$ ($\varepsilon_c^{(1)} = \varepsilon_s^{(1)} = 0.03$), and as $N(1)$ increases, the resonance amplitude decreases and may even disappear.

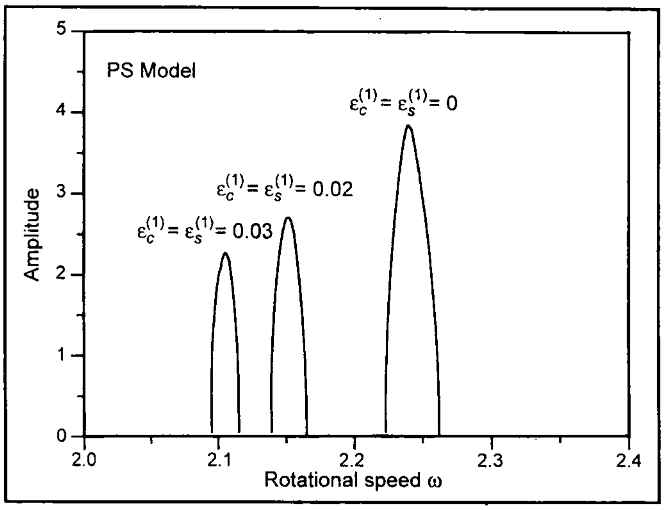

Figure 9. 1/2-Order subharmonic resonance with nonlinearity $N(1)$.

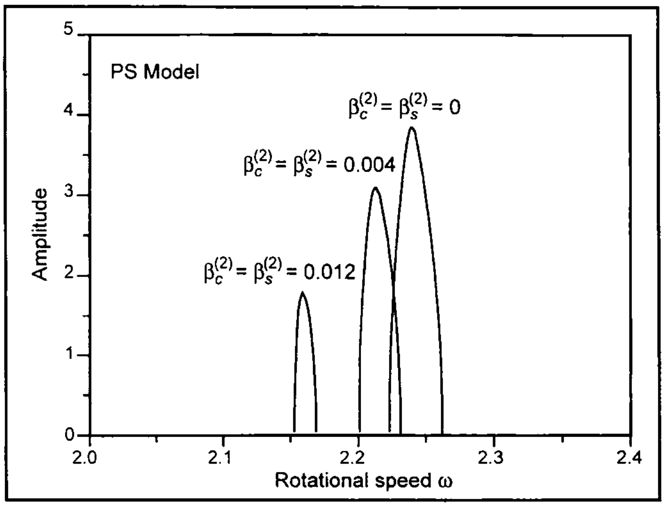

Figure 10. 1/2-Order subharmonic resonance with nonlinearity $N(2)$.

Figure 10 shows the 1/2-order subharmonic resonance curve for the case with symmetrical nonlinearity $N(2)$. In this case, the resonance curve shifts to the lower speed side and the amplitude decreases and also may disappear as $N(2)$ increases.

4.2. Harmonic Resonance at Major Critical Speed

Assumption made for the approximate solution. In the neighbourhood of the rotational speed ω_c, where the relationship $p_f = \omega$ holds in Fig. 11, a harmonic resonance at the major critical speed occurs. If we assume the solution has the same form as Eq. (11) and we use a similar procedure, we can obtain the following expressions for $P = P_0$ and $\beta = \beta_0$:

$$M\sin(\alpha - \beta_0) = c\omega P_0 - \Delta P_0 \sin 2\beta_0 + \varepsilon_2(P_s^2 + 0.5M_0^2)\cos\beta_0 + \varepsilon_4(P_s^4 + 3M_0^2P_s^2 + 0.375M_0^4)\cos\beta_0;$$

and

$$M\cos(\alpha - \beta_0) = GP_0 + \Delta P_0 \cos 2\beta_0 + \varepsilon_2(P_s^2 + 0.5M_0^2)\sin\beta_0 + \varepsilon_4(P_s^4 + 3M_0^2P_s^2 + 0.375M_0^4)\sin\beta_0 + 4\varepsilon_s^{(1)}M_0P + 4\beta^{(0)}P_0^3 + \left(8\beta^{(0)} - 6\beta_c^{(2)}\right)M_0^2P_0, \quad (13)$$

where, $P_s = P\sin\beta_0$ and $G = G(\omega) = 1 + i_p\omega^2 - \omega^2$. The equations include the nonlinear components $N(1)\,(\varepsilon_s^{(1)})$, $N(2)\,(\beta_c^{(2)})$ and $N(0)\,(\beta^{(0)})$.

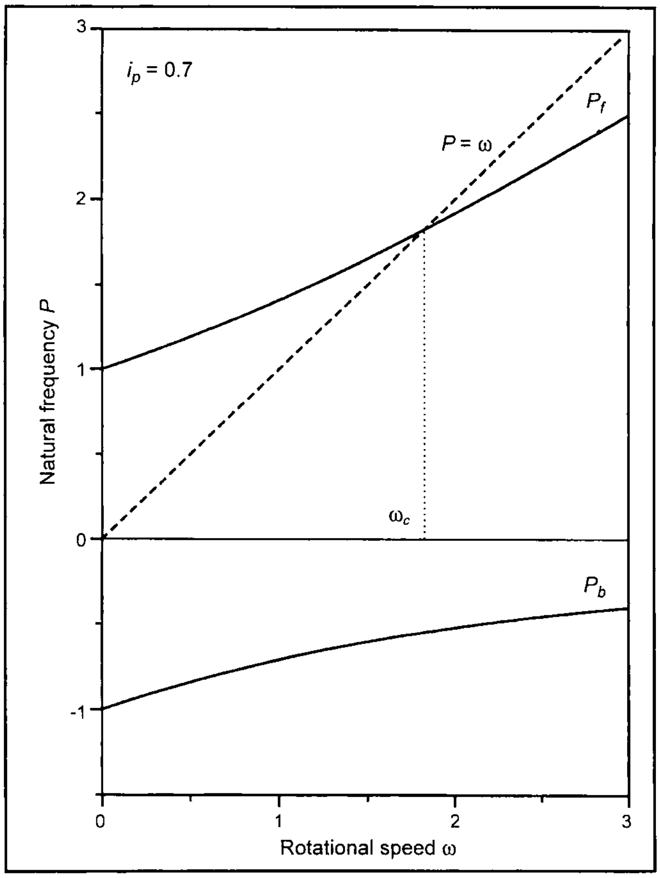

Figure 11. $p - \omega$ diagram ($i_p = 0.7$).

Resonance curves for a cracked rotor in a linear rotor system. The harmonic resonance curves resulting from a power series approximation of a cracked rotor due to a crack have been given in published papers[19,20]. In the case of a cracked rotor without nonlinear supports, an unstable region exists when an unbalance is located on the same side as the crack, i.e., $\alpha = 90°$. However, when an unbalance is located in the opposite side to the crack, i.e., $\alpha = 270°$, there is no unstable region.[20]

Resonance curves for a cracked rotor in a nonlinear rotor system. The harmonic resonance curves for a cracked rotor with nonlinear supports are shown in Figs. 12-14, where the parameters $\tau = 0.1, i_p = 0.7, c = 0.02, M_0 = -1.0, \Delta = 0.05$, $\varepsilon_2 = -0.05$, and $\varepsilon_4 = 0.001$. In order to compare these results to the results of numerical simulations, we also represent the results of numerical simulations in the figures included in this section.

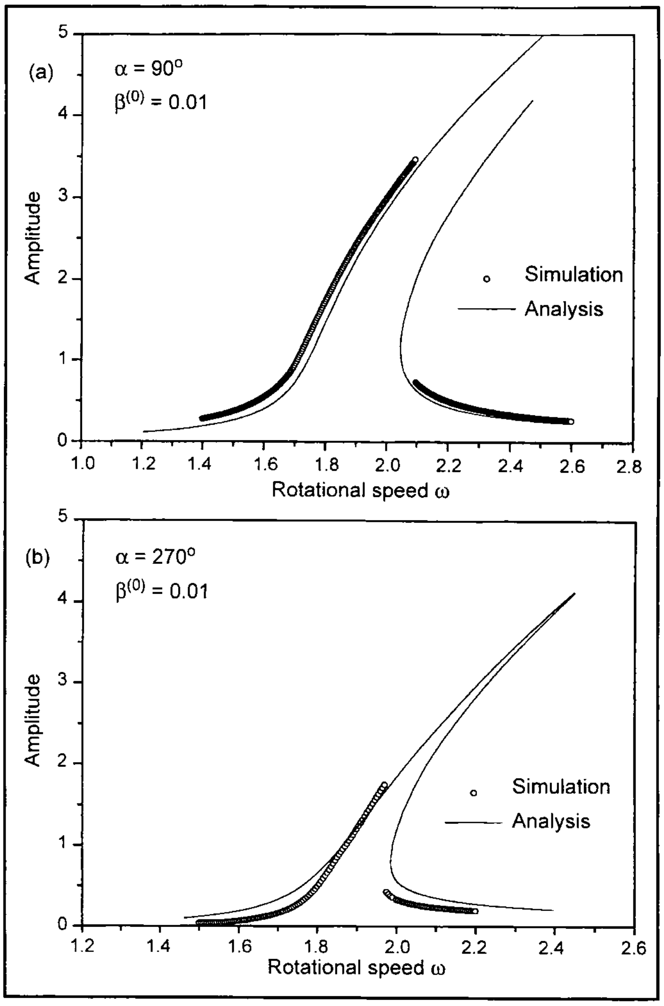

Figure 12. Harmonic resonance curve with nonlinearity $N(0)$.

Figure 12(a) shows the resonance curve for a cracked rotor with symmetrical nonlinearity $N(0)\,(\beta^{(0)} \neq 0)$ when $\alpha = 90°$. The resonance curves incline to the higher speed side and the unstable region which exists due to a crack may disappear.

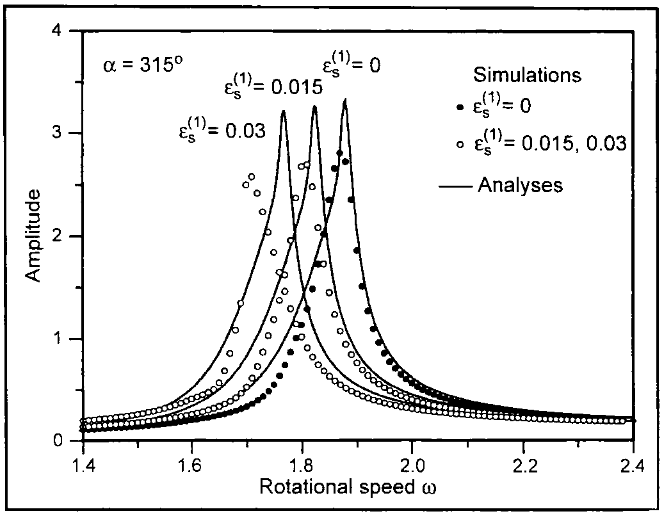

Figure 13. Harmonic resonance curve with nonlinearity $N(1)$.

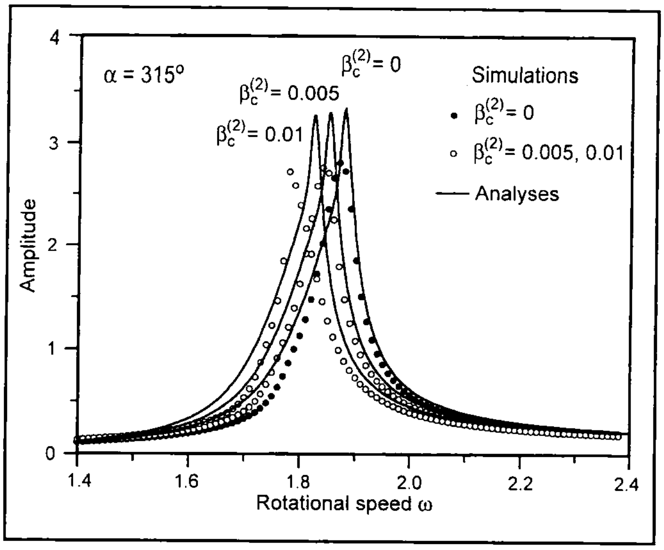

Figure 14. Harmonic resonance curve with nonlinearity $N(2)$.

Figure 12(b) shows the resonance curve for a cracked rotor with symmetrical nonlinearity $N(0)$ ($\beta^{(0)} \neq 0$) when $\alpha = 270°$. The resonance curves incline to the higher speed side and become like those of a hard spring.

Figure 13 shows the results for the case with unsymmetrical nonlinearity $N(1)(\varepsilon_s^{(1)} \neq 0)$ from numerical simulations and theoretical solutions when $\alpha = 315°$. In this case, the resonance curves shift to the lower speed side and the resonance amplitude decreases as $N(1)$ increases.

Figure 14 shows the resonance curves for a cracked rotor with symmetrical nonlinearity $N(2)(\beta_c^{(2)} \neq 0)$ when $\alpha = 315°$. In this case, the resonance curves shift to the lower speed side as $N(2)$ increases.

This paper investigates the vibrational behaviour of a cracked rotor with nonlinear supports for the purpose of detecting cracks in rotating shafts. The above results show that the results of theoretical solutions obtained from a PS model agree well qualitatively with the results of numerical simulations made with a PWL model.

Crack detection is also an important problem in the condition monitoring of rotating machinery. An early warning at the occurrence of a rotor crack can considerably extend the durability of machinery and increase its reliability. The detection of a crack in its early stages may save the rotor for continued use after repair. For detecting a crack in early stages in rotating shafts, many methods have been used to develop the on-line crack detection and monitoring techniques. These include vibration signature analysis, acoustic emission, and so on.[23,24,32] However, crack detection methods usually are based on signal analysis, and use information from vibration signals.

The vibration analysis techniques, which use PWL and PS models in this paper are based on a cracked rotor system with nonlinear supports. The techniques are advanced and can be developed to establish unique characteristic signatures to detect cracks in such nonlinear rotor systems.

In many practical rotor systems, nonlinear characteristics exist due to the rotor supports. Therefore, it is necessary to distinguish between the vibrational behaviour of a cracked rotor in a rotor system with nonlinear supports and those in a rotor system with linear supports. The results clarify the vibrational behaviour in these two rotor systems and show that the nonlinear components due to bearing supports have a large influence on the amplitude, position and shape of resonance curves due to a crack. These results are useful for conducting further studies to develop a fault diagnosis system for the detecting of rotor cracks.

5. CONCLUSIONS

This paper gives a detailed investigation of the dynamic behaviour of the harmonic resonance and the 1/2-order subharmonic resonance of a cracked rotor and establishes a clear relation between the resonance and angular positions of the unbalance of a cracked rotor. The results will be for making an assessment to identify and locate a crack in a cracked rotor system using these resonance phenomena.

This paper has investigated the dynamic behaviour of a cracked rotor with nonlinear supports due to different angular positions of an unbalance. The approaches include both a piecewise linear model and a power series model for modelling crack stiffness characteristics. The results obtained from theoretical solutions of a PS model up to the fourth order agree qualitatively with those obtained from numerical simulations with a PWL model.

The dynamic behaviours of cracked rotors with nonlinear supports are significantly different from those of cracked rotors with linear supports and are summarised below.

In a cracked rotor system with linear supports, the 1/2-order subharmonic resonance is almost independent of the angular positions of an unbalance. However, in a cracked rotor system with nonlinear supports, the amplitude and position of the 1/2-order subharmonic resonance are dependent on the angular positions of an unbalance. When a cracked rotor has unsymmetrical nonlinearity $N(1)$ or symmetrical nonlinearity $N(2)$, the resonance amplitudes have different magnitudes for different angular positions of an unbalance.

When the nonlinearity $N(1)$ or $N(2)$ become larger, the amplitudes of the 1/2-order subharmonic resonance become smaller or zero and the resonance positions shift to the lower speed side. In the case that the bearing supports have a larger nonlinear term $N(1)(\varepsilon_c^{(1)} = \varepsilon_s^{(1)} = 0.03)$, the resonance does not exist at all for $\alpha = 135°, 180°, 225°$. In the case when the bearing supports have a larger nonlinear term $N(2)(\beta_c^{(2)} = \beta_s^{(2)} = 0.012)$, the resonance does not exist either for $\alpha = 45°$, $315°$.

The angular positions of an unbalance have a significant influence on the unstable region at the major critical speed. In a cracked rotor system with linear supports, the unstable region at the major critical speed exists when $\alpha = 45°, 90°, 135°, 180°, 225°$. However, in the case of a cracked rotor with nonlinear supports $N(1)$, the unstable region may not exist with those same angular positions of the unbalance.

The nonlinearity $N(1)$ and $N(2)$ significantly affect the major critical speed. The position of harmonic resonance depends on the magnitudes of $N(1)$ and $N(2)$.

The symmetrical nonlinearity $N(0)$ has an influence on the shapes of the resonance curves. In the case when an unbalance is located at the same side as a crack, i.e., $\alpha = 90°$, the harmonic resonance inclines towards the higher speed side and the unstable region due to a crack may disappear. In the case that an unbalance is located at the opposite side from a crack, i.e., $\alpha = 270°$, the harmonic resonance inclines towards the higher speed side.

REFERENCES

[1] Dimarogonas, A.D., and Papadopoulos, C.A. *Analytical Methods in Rotor Dynamics*, London: Applied Science Publishers, (1983).

[2] Wauer, J. On the dynamics of cracked rotors: A literature survey, *Appl. Mech. Rev.*, **143** (1), 13-17, (1990).

[3] Gasch, R. A survey of the dynamic behaviour of a simple rotating shaft with a transverse crack, *J. Sound Vib.*, **160** (2), 313-332, (1993).

[4] Dimarogonas, A.D. Vibration of cracked structures: a state of the art review, *Engineering Fracture Mechanics*, **55**, 831-857, (1996).

[5] Gasch, R. Dynamic behaviour of a simple rotor with a cross-sectional crack, *Vibrations in Rotating Machinery*, Institution of Mechanical Engineers, London, 123-128, (1976).

[6] Gasch, R. Dynamisches Verhalten des Laval-Läufers mit angerissenem Wellenquerschnitt, *VDI-Berichchte*, No. 269, VDI-Verlag, Düsseldorf, 183-188, (1976).

[7] Henry, T.A., and Okah-Avae, B.E. Vibrations in cracked shafts, *Vibrations in Rotating Machinery*, Institution of Mechanical Engineers, London, 15-19, (1976).

[8] Mayes, I.W., and Davies, W.G.R. The vibrational behaviour of a rotating shaft system containing a transverse crack, *Vibrations in Rotating Machinery*, Institution of Mechanical Engineers, London, 53-65, (1976).

[9] Mayes, I.W., and Davies, W.G.R. Analysis of the response of a multi-rotor-bearing system containing a transverse crack in a rotor, *J. Vib Acous. Stress Reliab Des.*, **106**, 139-145, (1984).

[10] Davies, W.G.R., and Mayes, I.W. The vibrational behaviour of a multi-shaft, multi-bearing system in the presence of a propagating transverse crack, *J. Vib Acous. Stress Reliab Des.*, **106**, 146-153, (1984).

[11] Grabowski, B. The vibrational behaviour of a turbine rotor containing a transverse crack, *J. Mech Des.*, **102**, 140-146, (1980).

[12] Grabowski, B. The vibrational behaviour of a rotating shaft containing a transverse crack, *Dynamics of Rotors-Stability and System Identification*, CISM courses and lectures, No. 273, Springer, New York, 423-465, (1984).

[13] Dimarogonas, A.D., and Papadopoulos, C.A. Vibration of a cracked shafts in bending, *J. Sound Vib.*, **91**, 583-593, (1983).

[14] Papadopoulos, C.A., and Dimarogonas, A.D. Coupled longitudinal and bending vibrations of a rotating shaft with an open crack, *J. Sound Vib.*, **117**, 81-93, (1987).

[15] Papadopoulos, C.A., and Dimarogonas, A.D. Stability of cracked rotor in the coupled vibration mode, *J. Vib Acous. Stress Reliab Des.*, **110**, 356-359, (1988).

[16] Sekhar, A.S., and Balaji, P. Dynamic analysis of a rotor system considering a slant crack in the shaft, *J. Sound Vib.*, **208** (3), 457-474, (1997).

[17] Gasch, R., Person, M., and Weitz, B. Dynamic behaviour of the Laval rotor with a cracked hollow shaft - a comparison of cracked model, *Vibrations in Rotating Machinery*, Institution of Mechanical Engineers, London, 463-472, (1988).

[18] Tamura, A., Iwata, Y., and Sato, H. Unstable vibration of a rotor with a transverse crack, *Vibrations in Rotating Machinery*, Institution of Mechanical Engineers, London, 647-653, (1988).

[19] Ishida, Y., Ikeda, T., Yamamoto, T., and Masuda, N. Vibrations of a rotating shaft containing a transverse crack, *JSME Int J.*, Series III, **31** (1), 22-29, (1988).

[20] Ishida, Y., Yamamoto, T., and Hirokawa, K. Vibrations of a rotating shaft containing a transverse crack: Major critical speed of horizontal shaft, *Transactions of the JSME*, (C), **58** (551), 26-33, (1992).

[21] Nelson, H.D., and Nataraj, C. The dynamics of a rotor system with a cracked shaft, *J. Vib Acous. Stress Reliab Des.*, **108**, 189-196, (1986).

[22] Meng, G., and Hahn, E.J. Dynamic response of a cracked rotor with some comments on crack detection, *J. Engineering for Gas Turbines and Power*, **119**, 447-455, (1997).

[23] Iman, I., Azzaro, S.H., Bankert, R.J., and Scheibel, J. Development of an on-line rotor crack detection and monitoring system, *J. Vib Acous. Stress Reliab Des.*, **111**, 241-250, (1989).

[24] Ratan, S., Baruh, H., and Rodriguez, J. On-line identification and location of rotor cracks, *J. Sound Vib.*, **194** (1), 67-82, (1996).

[25] Chan, R.K.C., and Lai, T.C. Digital simulation of a rotating shaft with a transverse crack, *Applied Mathematical Modeling*, **19** (7), 411-420, (1995).

[26] Ehrich, F.F. High order subharmonic response of high speed rotor in bearing clearance, *J. Vib Acous. Stress Reliab Des.*, **110**, 9-16, (1988).

[27] Ehrich, F.F. Nonlinear phenomena in dynamic response of rotors in anisotropic mounting systems, *Special 50th Anniversary Design Issue*, **117**, 154-161, (1995).

[28] Yamamoto, T., and Ishida, Y. *Linear and Nonlinear Rotordynamics: Modern Treatment and Application*, Corona Publishing CO., LTD, Tokyo, Japan, (in Japanese), (2001).

[29] Yamamoto, T., and Ishida, Y. *Linear and Nonlinear Rotordynamics: A Modern Treatment with Applications*, John Wiley and Sons, Inc., USA, (2001).

[30] Okah-Avae, B.E. Analogue computer simulation of a rotor system containing a transverse crack, *Simulation*, **31** (6), 193-198, (1978).

[31] Okah-Avae, B.E., and Mbonu, O.J. Computer analog digital simulation of a complex mechanical system, *Simulation*, **37** (2), 47-53, (1981).

[32] Müller, P.C., Bajkowski, J., and Söffker, D. Chaotic motions and fault detection in a cracked rotor, *Nonlinear Dynamics*, **5**, 233-254, (1994).

[33] Meng, G., and Gasch, R. Stability and stability degree of a cracked flexible rotor supported on journal bearings, *J. Vib Acous.*, **122**, 116-125, (2000).

[34] Ishida, Y., and Lu, F. Influence of static nonlinearity to resonances due to a crack, *Seventh conference on nonlinear vibration, stability, and dynamics of structures*, Blacksburg, Virginia, USA, (1998).

[35] Lu, F., and Zhang, N. Vibrations of a cracked rotor in a nonlinear rotor system, *Seventh International Congress on Sound and Vibration*, Garmisch-Partenkirchen, Germany, **V**, 2875-2882, (2000).

[36] Yamamoto, T., Yasuda, K., and Nagasaka, I. Ultra-subharmonic oscillations in a nonlinear vibratory system, *Bulletin of the JSME*, **19** (138), 1442-1447, (1976).

[37] Yamamoto, T. and Ishida, Y. Nonlinear oscillations in a rotating shaft system, *Second conference on nonlinear vibration, stability, and dynamics of structures*, Blacksburg, Virginia, USA, (1988).